Online Leader Selection for Collective Tracking and Formation Control: The Second-Order Case

Antonio Franchi, *Senior Member, IEEE*, Paolo Robuffo Giordano, *Senior Member, IEEE*, and Giulia Michieletto, *Member, IEEE*

***Abstract*—In this paper, we deal with a double control task for a group of interacting agents that have second-order dynamics. Adopting the leader–follower paradigm, the given multiagent system is required to maintain a desired formation and to collectively track a velocity reference provided by an external source only to a single agent at time, called the "leader." We prove that it is possible to optimize the group performance by persistently selecting *online* the leader among the agents. To do this, we first define a suitable error metric that is able to capture the tracking performance of the multiagent group while maintaining a desired formation through a (even time-varying) communication-graph topology. Then, we show that this depends on the algebraic connectivity and on the maximum eigenvalue of the Laplacian matrix of a special *directed graph* depending on the selected leader. By exploiting these theoretical results, we finally design a fully distributed adaptive procedure that is able to periodically select *online* the *optimum leader* among the neighbors of the current one. The effectiveness of the proposed solution against other possible strategies is confirmed by numerical simulations.**

***Index Terms*—Decentralized control, distributed agent systems, distributed algorithms, mobile agents, multiagent systems.**

I. Introduction

FOR multiagent systems, the tracking of a collective motion constitutes a well-studied problem in both the control and agentic communities (see, e.g., the recent [1] but also [2]–[4]). Most of the proposed tracking algorithms rely upon the *leader–follower paradigm*, a very popular technique [5]–[12], which envisages the presence of a special agent, referred to as the *leader*, that has access to the reference motion (often provided by an external source) to be propagated to the whole group. This approach arises as a very powerful tool in real applications, mainly because in many situations, it is unfeasible to communicate at the same time with all agents in the group especially if they are geographically distributed and the available bandwidth is limited.

Within the multiagent context, the leader–follower solutions have to guarantee the propagation of the reference motion and its tracking with the smallest possible error/delay by means of proper local actions. For this reason, the selection of the leader plays an important role, and the literature distinguishes between *static* and *online* leader selection. In the first case, the leader is constantly assumed to be a certain agent within the group chosen at the beginning of the task by the whole multiagent system. Contrarily, when adopting the online selection, the leader is left free to change over time.

Related works: Both in the static and online case, the leader selection generally rests upon the optimization of a suitable index. For example, the authors of [13] have addressed the static leader election task accounting for the maximization of the network coherence, defined as the ability of the consensus-network to reject stochastic disturbances, while in [14], the *harmonic influence centrality* measure is used to quantify the influence of a node on the opinion of the global network. Allowing for the presence of multiple (static) leaders, in [15], a fully distributed strategy is described to select the minimum set of leaders that ensures the structural controllability of the resulting communicating system, whereas a prespecified number of leaders is assumed in [16], focusing on the computation of bounds on the global optimal value in large stochastically forced consensus networks. A similar scenario is considered in [17] where the *K-leader selection problem* (standard static leader selection issue) is investigated in ring and path graphs assuming that leaders are noise-free and followers obey noisy consensus dynamics. The authors of [18] instead evaluate the effect of noise-corrupted leaders in the network performance through the definition of the joint centrality of a set of nodes. Finally, in [19], the combinatorial nature of the problem of choosing k leaders among n agents is analyzed, showing that the task can be efficiently faced via a semidefinite program, once a suitable sequence of relaxations is applied.

Although the literature about an online leader selection is more limited, the authors of [20] have addressed this problem by investigating the instantaneous impact of the (time-varying) leaders on the remaining agents through the notion of manipulability. In [21], instead, both the total and the maximum variance of the deviation from a desired trajectory are taken into account to face the so-called *in-network leader selection problem* designing a self-stabilizing algorithm that, after a topology

Manuscript received May 7, 2018; revised October 16, 2018; accepted December 8, 2018. Date of publication January 4, 2019; date of current version December 17, 2019. This work was supported by the ANR, Project ANR-17-CE33-0007 MuRoPhen. Recommended by Associate Editor F. Zhang. *(Corresponding author: Antonio Franchi.)*

A. Franchi is with the LAAS-CNRS, Université de Toulouse, CNRS, Toulouse 31400, France (e-mail: antonio.franchi@laas.fr).

P. Robuffo Giordano is with CNRS, Univ Rennes, Inria, IRISA, Rennes, France (e-mail: prg@irisa.fr).

G. Michieletto is with theDepartment of Information Engineering, University of Padova, Padova 35100, Italy (e-mail: giulia.michieletto@unipd.it).

Digital Object Identifier 10.1109/TCNS.2019.2891011

change, ensures network stability until the online determination of the optimal leader for the new topology. Such an approach rests on agents' cooperation: the determination of a distributed control protocol guaranteeing the leadership uniqueness constitutes the main challenge of both static and online leader selection. Within the static context, this issue has been tackled in [22] by using explicit message passing among the formation, while a fault detection strategy without explicit communication need is exploited in [23]. Allowing for a time-varying leadership, the leader identity becomes an additional degree of freedom that has to be handled over time by the network in a distributed manner, limiting the selection duration and its computational burden.

Contributions: Different from all of the aforementioned works in [24], we have proposed performing the online leader selection to simultaneously optimize the collective tracking performance from an external source and the maintenance of a desired formation shape. The goal of this paper is to considerably extend the results achieved in [24] by considering a more complex dynamics for the multiagent group: while in [24], the agents behave as first-order systems, we now consider second-order dynamics, thus assuming the linear accelerations as a control input. The presentation of the contributions follows the same structure of [24] to clearly highlight the differences arising from the adoption of the double-integrator dynamic model. These are clearly stated at the end of this paper and mainly derive from the fact that the metrics introduced in [24] are not valid anymore in the second-order case.

For a group of agents modeled as second-order systems, we first formalize the problem of tracking an external reference motion while maintaining a desired formation assuming that the leader identity and the interaction graph topology can be both time-varying. Then, we analyze the effect of changing leadership to accomplish the formation control task by showing a direct dependence of the convergence of a suitably defined tracking error on the leader identity. Finally, we propose a new distributed leader election procedure whose effectiveness is validated by means of numerical simulations.

II. Modeling of Collective External Reference Tracking and Desired Formation Maintenance

The first contribution of this paper is a set of results regarding the modeling of a multiagent scenario consisting of a group of N mobile agents equipped with communication, sensing, and computation capabilities. Each agent i, $i \in \{1, \ldots, N\}$ of the group is considered as a point mass in $\mathbb{R}^d$, with $d \in \{2, 3\}$. The ith agent position is denoted by $\mathbf{p}_i \in \mathbb{R}^d$ and its linear velocity by $\dot{\mathbf{p}}_i = \mathbf{v}_i \in \mathbb{R}^d$. The set of the linear accelerations $\{\dot{\mathbf{v}}_i\}_{i=1}^N$ will be considered as the control input set in the following development.

An undirected graph $\mathcal{G}$, called the *interaction graph*, describes the interagent sensing and communication capabilities so that the corresponding adjacency matrix $\mathbf{A} \in \{0, 1\}^{N \times N}$ is such that $[\mathbf{A}]_{ij} = 1$ if agents i and j, $j \neq i$, can communicate and measure their relative position $\mathbf{p}_{ij} = \mathbf{p}_i - \mathbf{p}_j \in \mathbb{R}^d$, and $[\mathbf{A}]_{ij} = 0$ otherwise, $\forall\, i, j \in \{1, \ldots, N\}$. The *neighborhood* $\mathcal{N}_i = \{j \mid A_{ij} = 1\}$ of the node i in $\mathcal{G}$ denotes thus the set of agents with which the ith one can interact. The cardinality of this set represents the *degree* of the ith agent, which, in turn, corresponds to the ith element in the main diagonal of $\mathbf{D} = \mathrm{diag}(\mathbf{A}\mathbf{1}) \in \mathbb{R}^{N \times N}$, that is, in the diagonal matrix associated with the vector $\mathbf{A}\mathbf{1}$ with $\mathbf{1} \in \mathbb{R}^N$ representing a column vector of all ones. The degree matrix $\mathbf{D}$ contributes to the definition of the Laplacian matrix $\mathbf{L} \in \mathbb{R}^{N \times N}$ of $\mathcal{G}$, that is, $\mathbf{L} = \mathbf{D} - \mathbf{A}$. We assume that the second smallest eigenvalue λ_2 of $\mathbf{L}$ (algebraic connectivity of $\mathcal{G}$) is positive or, equivalently, that the Laplacian matrix has rank $N - 1$. This condition is guaranteed by the existence of at least one communication path (i.e., a sequence of edges) for any pair of agents in the group, so that the graph $\mathcal{G}$ is connected.

In this paper, the multiagent swarm is required to track a collective motion command provided to the group by an external "entity" (such as another agent, a planner, or a human operator), referred to as the *reference source*. We assume that this transmits a certain velocity reference $\mathbf{u}_r \in \mathbb{R}^d$, which is supposed to be a piecewise constant function with period T_r (*reference command period*). In addition, we assume that the current value of $\mathbf{u}_r$ is communicated by the reference source to *only one* agent of the group at a time, called the "current" *leader* and denoted by the possibly time-varying index l.

The connectivity assumption on the interaction network ensures that the reference velocity can be transmitted to the whole group of agents by exploiting a multihop propagation algorithm. Without focusing on particular propagation schemes, we consider the following consensus-based strategy:

$$\hat{\mathbf{u}}_l = \mathbf{u}_r \tag{1}$$

$$\dot{\hat{\mathbf{u}}}_i = -k_u \sum_{j \in \mathcal{N}_i} (\hat{\mathbf{u}}_i - \hat{\mathbf{u}}_j) \quad \forall i \neq l \tag{2}$$

where $\hat{\mathbf{u}}_i \in \mathbb{R}^d$ is the estimation of $\mathbf{u}_r$ performed by the ith agent, while the positive scalar gain k_u tunes the algorithm convergence speed, allowing to model both fast or slow propagation technologies, for example, high-bandwidth local-area networks (LANs) or ultrasonic underwater communication, respectively. Note that for the leader, $\hat{\mathbf{u}}_l = \mathbf{u}_r$ since the reference is directly available.

To compactly rewrite the propagation model (1) and (2), we introduce the "in-degree" Laplacian matrix $\mathbf{L}_l \in \mathbb{R}^{N \times N}$ of the directed graph $\mathcal{G}_l$, that is obtained from $\mathcal{G}$ by removing all of the ingoing-edges of l. In other words, the matrix $\mathbf{L}_l$ is derived from $\mathbf{L}$ by zeroing its lth row so that

$$\mathbf{L}_l = \begin{bmatrix} \mathbf{M}_{l,1} & \boldsymbol{\ell}_{l,1} & \mathbf{M}_{l,2} \\ \mathbf{0}^\top & 0 & \mathbf{0}^\top \\ \mathbf{M}_{l,3} & \boldsymbol{\ell}_{l,2} & \mathbf{M}_{l,4} \end{bmatrix} \tag{3}$$

where $\mathbf{M}_{l,1}$, $\mathbf{M}_{l,2}$, $\mathbf{M}_{l,3}$, $\mathbf{M}_{l,4}$, $\boldsymbol{\ell}_{l,1}$, $\boldsymbol{\ell}_{l,2}$, and $\mathbf{0}$ are matrices and column vectors of proper dimensions. By introducing also the matrix $\mathbf{G}_l = -(\mathbf{L}_l \otimes \mathbf{I}_d) \in \mathbb{R}^{dN \times dN}$ where $\otimes$ denotes the Kronecker product, and the vector $\hat{\mathbf{u}} = [\hat{\mathbf{u}}_1^\top, \ldots, \hat{\mathbf{u}}_N^\top]^\top \in \mathbb{R}^{dN}$, the estimation dynamics (1) and (2) can be compactly rewritten as

$$\dot{\hat{\mathbf{u}}} = -k_u (\mathbf{L}_l \otimes \mathbf{I}_d) \hat{\mathbf{u}} = k_u \mathbf{G}_l \hat{\mathbf{u}}. \tag{4}$$

As a further task, the agents group needs to maintain a desired formation shape defined through the set of constant (absolute) positions $\mathbf{d} = [\mathbf{d}_1^\top, \ldots, \mathbf{d}_N^\top]^\top \in \mathbb{R}^{dN}$. Based on the actuation

and sensing properties of the agents, this goal can be accomplished through several control strategies. For the sake of model generality, we here consider a classical consensus-like solution applied to second-order agents, namely

$$\dot{\mathbf{p}}_i = \mathbf{v}_i \tag{5}$$

$$\dot{\mathbf{v}}_l = b(\mathbf{u}_r - \mathbf{v}_l) \tag{6}$$

$$\dot{\mathbf{v}}_i = b(\hat{\mathbf{u}}_i - \mathbf{v}_i) - k_p \sum_{j \in \mathcal{N}_i} (\mathbf{p}_{ij} - \mathbf{d}_{ij}) \quad \forall i \neq l \tag{7}$$

where $\mathbf{d}_{ij} = \mathbf{d}_i - \mathbf{d}_j \in \mathbb{R}^d$ represents the desired relative position between agents i and j. The positive scalar gains b and k_p determine the velocity tracking performances and the "stiffness" of the formation control, that is, how strongly the agents will react to deviations from their desired formation. The convergence toward the desired configuration is guaranteed by the connectivity of the network interaction graph [25].

Exploiting the matrix $\mathbf{G}_l$ (previously introduced) and the vectors $\mathbf{p} = [\mathbf{p}_1^\top, \ldots, \mathbf{p}_N^\top]^\top \in \mathbb{R}^{dN}$, $\mathbf{v} = [\mathbf{v}_1^\top, \ldots, \mathbf{v}_N^\top]^\top \in \mathbb{R}^{dN}$, and $\mathbf{d} = [\mathbf{d}_1^\top, \ldots, \mathbf{d}_N^\top]^\top \in \mathbb{R}^{dN}$, the complete agents group dynamics can be shortened as follows:

$$\dot{\mathbf{p}} = \mathbf{v} \tag{8}$$

$$\dot{\mathbf{v}} = b(\hat{\mathbf{u}} - \mathbf{v}) + k_p \mathbf{G}_l(\mathbf{p} - \mathbf{d}). \tag{9}$$

Let us then introduce the *formation tracking error*, the *velocity tracking error,* and the *velocity estimation error*, namely

$$\mathbf{e}_\mathbf{p} = (\mathbf{p} - \mathbf{1} \otimes \mathbf{p}_l) - (\mathbf{d} - \mathbf{1} \otimes \mathbf{d}_l) \tag{10}$$

$$\mathbf{e}_\mathbf{v} = \mathbf{v} - \mathbf{1} \otimes \mathbf{v}_l \tag{11}$$

$$\mathbf{e}_{\hat{\mathbf{u}}} = \hat{\mathbf{u}} - \mathbf{1} \otimes \mathbf{u}_r. \tag{12}$$

The first one provides a measure of accuracy in tracking and maintaining the desired formation shape encoded in $\mathbf{d}$, while the second and the third ones represent, respectively, the tracking accuracy of the leader velocity $\mathbf{v}_l$, and the error in estimation the reference $\mathbf{u}_r$.

Using the properties $b(\hat{\mathbf{u}} - \mathbf{v}) - \mathbf{1} \otimes \dot{\mathbf{v}}_l = b(\mathbf{e}_{\hat{\mathbf{u}}} - \mathbf{e}_\mathbf{v}), \dot{\mathbf{e}}_\mathbf{p} = \mathbf{e}_\mathbf{v}$, $\mathbf{G}_l(\mathbf{p} - \mathbf{d}) = \mathbf{G}_l \mathbf{e}_\mathbf{p}$, and taking into account (4), (8), and (9), the dynamics of the overall error $\mathbf{e} = [\mathbf{e}_\mathbf{p}^\top \ \mathbf{e}_\mathbf{v}^\top \ \mathbf{e}_{\hat{\mathbf{u}}}^\top]^\top$ takes the expression

$$\dot{\mathbf{e}} = \begin{bmatrix} \mathbf{0} & \mathbf{I}_{dN} & \mathbf{0} \\ k_p \mathbf{G}_l & -b\mathbf{I}_{dN} & b\mathbf{I}_{dN} \\ \mathbf{0} & \mathbf{0} & k_u \mathbf{G}_l \end{bmatrix} \mathbf{e} \tag{13}$$

where the reference velocity is assumed constant ($\dot{\mathbf{u}}_r = \mathbf{0}$).

The system (13) presents some interesting properties whose role is fundamental to derive the main contributions of this paper. In this perspective, we first define

$$\boldsymbol{\ell}_l = [\boldsymbol{\ell}_{l,1}^\top \ \boldsymbol{\ell}_{l,2}^\top]^\top \in \mathbb{R}^{N-1} \tag{14}$$

$$\mathbf{M}_l = \begin{bmatrix} \mathbf{M}_{l,1} & \mathbf{M}_{l,2} \\ \mathbf{M}_{l,3} & \mathbf{M}_{l,4} \end{bmatrix} \in \mathbb{R}^{(N-1)\times(N-1)} \tag{15}$$

where $\mathbf{M}_l$ is the matrix obtained from $\mathbf{L}_l$ by removing its lth row and column. Moreover, we report here the following (known) facts important for the next developments.

Property 1 (Property 1 in [24]): If graph $\mathcal{G}$ is connected, the following properties hold:

1) $\mathbf{L}_l \mathbf{1} = \mathbf{0}, \forall l = 1, \ldots, N$;
2) $\mathbf{M}_l \mathbf{1} = (\mathbf{1}^\top \mathbf{M}_l)^\top = -\boldsymbol{\ell}_l$;
3) $\mathbf{M}_l$ is symmetric and positive definite;
4) $\sigma(\mathbf{L}_l) = \sigma(\mathbf{M}_l) \cup \{0\}$, where $\sigma(\mathbf{S})$ represents the spectrum of a square matrix $\mathbf{S}$.

A consequence of this property is that the matrix $\mathbf{L}_l$ has N *real* non-negative eigenvalues even though it is not symmetric. Let $\sigma(\mathbf{L}_l) = \{\lambda_{i,l}, i = 1, \ldots, N \mid 0 = \lambda_{1,l} \leq, \ldots, \leq \lambda_{N,l}\}$ and $\sigma(\mathbf{L}) = \{\lambda_i, i = 1, \ldots, N \mid 0 = \lambda_1 \leq, \ldots, \leq \lambda_N\}$ be the spectrum of $\mathbf{L}_l$ and $\mathbf{L}$, then the following property holds.

Property 2 (Property 2 in [24]): For a graph $\mathcal{G}$ and an induced graph $\mathcal{G}_l$, it is $\lambda_{i,l} \leq \lambda_i$ for all $i = 1, \ldots, N$.

Property 2 descends from the Cauchy interlacing theorem applied to matrices $\mathbf{L}$ and $\mathbf{M}_l$ and it implies that if $\mathcal{G}$ is connected, then both $\lambda_2 > 0$ and $\lambda_{2,l} > 0$, where by analogy, we denote $\lambda_{2,l}$ as the "algebraic connectivity" of $\mathcal{G}_l$.

Given these premises, we conclude this behavioring section by formally proving the stability of the system (13).

Proposition 1: If graph $\mathcal{G}$ is connected, system (13) is asymptotically stable for any positive constants k_p, b, k_u. Furthermore, if

$$b > b_c = 2\sqrt{k_p \lambda_{N,l}} \quad \text{(critical damping)}$$

the system evolution has no oscillatory modes, where $\lambda_{N,l} = \max \sigma(\mathbf{M}_l)$, that is, the largest positive eigenvalue of $\mathbf{L}_l$. Finally, the rates of convergence of $[\mathbf{e}_\mathbf{p}^\top \ \mathbf{e}_\mathbf{v}^\top]^\top$ and $\mathbf{e}_{\hat{\mathbf{u}}}$ are dictated by

$$-\frac{b}{2} + \frac{1}{2}\sqrt{b^2 - 4k_p\lambda_{2,l}} \quad \text{and} \quad -k_u\lambda_{2,l}$$

respectively, where $\lambda_{2,l} = \min \sigma(\mathbf{M}_l)$, that is, the smallest positive eigenvalue of $\mathbf{L}_l$ (algebraic connectivity of $\mathcal{G}_l$).

Proof: Since $\mathbf{e}_{\mathbf{p},l} = \dot{\mathbf{e}}_{\mathbf{p},l} = \mathbf{e}_{\mathbf{v},l} = \dot{\mathbf{e}}_{\mathbf{v},l} = \mathbf{e}_{\hat{\mathbf{u}},l} = \dot{\mathbf{e}}_{\hat{\mathbf{u}},l} = \mathbf{0}$, the stability of (13) is determined by the real part of the eigenvalues of the $3(N-1) \times 3(N-1)$ matrix

$$\mathbf{R} = \begin{bmatrix} \mathbf{0} & \mathbf{I}_{(N-1)} & \mathbf{0} \\ -k_p\mathbf{M}_l & -b\mathbf{I}_{(N-1)} & b\mathbf{I}_{(N-1)} \\ \mathbf{0} & \mathbf{0} & -k_u\mathbf{M}_l \end{bmatrix} \otimes \mathbf{I}_d$$

that is required to be negative definite. Thanks to the properties of the Kronecker product, we can focus on the first matrix composing $\mathbf{R}$. Being a block upper triangular matrix, it is $\sigma(\mathbf{R}) = \sigma(\mathbf{R}_{11}) \cup \sigma(\mathbf{R}_{22})$, where

$$\mathbf{R}_{11} = \begin{bmatrix} \mathbf{0} & \mathbf{I}_{(N-1)} \\ -k_p\mathbf{M}_l & -b\mathbf{I}_{(N-1)} \end{bmatrix} \quad \text{and} \quad \mathbf{R}_{22} = -k_u\mathbf{M}_l.$$

The spectrum of $\mathbf{R}_{22}$ is clearly $\sigma(\mathbf{R}_{22}) = -k_u\sigma(\mathbf{M}_l) = \{-k_u\lambda_{2,l}, \ldots, -k_u\lambda_{N,l}\}$. On the other hand, for any eigenvalue $\mu_j, j \in \{1, \ldots, 2(N-1)\}$ of $\mathbf{R}_{11}$, it follows that:

$$\mathbf{R}_{11}\mathbf{v}_j = \mu_j \mathbf{v}_j \tag{16}$$

where $\mathbf{v}_j = [\mathbf{v}_{j,1}^\top \ \mathbf{v}_{j,2}^\top]^\top \in \mathbb{R}^{2(N-1)}$ is the unit-norm eigenvector of $\mathbf{R}_{11}$ associated with μ_j. Consider the matrix $(\mathbf{I}_2 \otimes \boldsymbol{w}_i^\top) \in \mathbb{R}^{2\times 2(N-1)}$, where $\boldsymbol{w}_i \in \mathbb{R}^{(N-1)}$ is the unit-norm eigenvector

of $\mathbf{M}_l$ associated with the eigenvalue $\lambda_{i,l}, i \in \{2,\dots,N\}$. Left-multiplying both sides of (16) with $(\mathbf{I}_2 \otimes \boldsymbol{w}_i^\top)$ and exploiting the symmetry of $\mathbf{M}_l$, we obtain

$$\underbrace{\begin{bmatrix} 0 & 1 \\ -k_p\lambda_{i,l} & -b \end{bmatrix}}_{\mathbf{R}_{\lambda_{i,l}}} \begin{bmatrix} \boldsymbol{w}_i^\top \mathbf{v}_{j,1} \\ \boldsymbol{w}_i^\top \mathbf{v}_{j,2} \end{bmatrix} = \mu_j \begin{bmatrix} \boldsymbol{w}_i^\top \mathbf{v}_{j,1} \\ \boldsymbol{w}_i^\top \mathbf{v}_{j,2} \end{bmatrix}.$$

Hence, μ_j must also be an eigenvalue of the 2×2 matrix $\mathbf{R}_{\lambda_{i,l}}$ for every $\lambda_{i,l} \in \sigma(\mathbf{M}_l)$, $i = 2,\dots,N$. This directly leads to

$$\mu_{2i-1} = -\frac{b}{2} + \frac{1}{2}\sqrt{b^2 - 4k_p\lambda_{i+1,l}} \tag{17}$$

$$\mu_{2i} = -\frac{b}{2} - \frac{1}{2}\sqrt{b^2 - 4k_p\lambda_{i+1,l}} \tag{18}$$

for $i = 1,\dots,N-1$. ■

Therefore, both the agent velocities $\mathbf{v}$ and the estimation vector $\hat{\mathbf{u}}$ asymptotically converge to the common reference velocity $\mathbf{u}_r$, while the agent positions $\mathbf{p}$ converge to the desired shape $\mathbf{1}\otimes\mathbf{p}_l + \mathbf{d} - \mathbf{1}\otimes\mathbf{d}_l$. Furthermore, the value of $\lambda_{2,l}$ directly affects the convergence rate of the three error vectors $\mathbf{e}_\mathbf{p}$, $\mathbf{e}_\mathbf{v}$, $\mathbf{e}_{\hat{\mathbf{u}}}$ over time. Since, for a given graph topology $\mathcal{G}$, $\lambda_{2,l}$ is determined by the *identity* of the leader in the group, it follows that maximization of $\lambda_{2,l}$ over the possible leaders results in faster convergence of the tracking error. This insight then motivates the online leader selection strategy detailed in the rest of this paper, where we will show that such maximization is actually only one of the ingredients for obtaining faster convergence through online leader selection.

III. Role of Leader in Tracking Performance

In this section, we provide a theoretical analysis of how the dynamics of the error vector is affected by changing the leader of the agents group at time $t_k = kT$ with $k \in \mathbb{N}$ and $T > 0$ (*leader election period*). Since it is reasonable to assume that the internal group communication is much faster than the reference source/leader interaction, we suppose $T \le T_r$ so that the velocity reference $\mathbf{u}_r$ remains constant between t_k and t_{k+1}. Hereafter, we denote the leader at time t_k with the index l_k.

Rewriting the dynamics of the velocity estimation (4) and of system (8) and (9) among consecutive sampling times, that is, during the interval $[t_k, t_{k+1})$, we obtain

$$\dot{\hat{\mathbf{u}}} = k_u \mathbf{G}_{l_k}\hat{\mathbf{u}}, \qquad t \in [t_k, t_{k+1}) \tag{19}$$

$$\dot{\mathbf{p}} = \mathbf{v}, \qquad t \in [t_k, t_{k+1}) \tag{20}$$

$$\dot{\mathbf{v}} = b(\hat{\mathbf{u}} - \mathbf{v}) + k_p \mathbf{G}_{l_k}(\mathbf{p} - \mathbf{d}), \qquad t \in [t_k, t_{k+1}) \tag{21}$$

with the following initial conditions where t_k^- coincides with the right extreme of the previous time interval[1]

$$\hat{\mathbf{u}}(t_k) = \hat{\mathbf{u}}(t_k^-) + (\bar{\mathbf{S}}_{l_k}\otimes\mathbf{I}_d)(\mathbf{1}\otimes\mathbf{u}_r(t_k) - \hat{\mathbf{u}}(t_k^-)) \tag{22}$$

$$\mathbf{p}(t_k) = \mathbf{p}(t_k^-) \tag{23}$$

$$\mathbf{v}(t_k) = \mathbf{v}(t_k^-). \tag{24}$$

[1]Formally, t_k^- coincides with the one-sided limit of time function approaches t_k "from below".

The matrix $\bar{\mathbf{S}}_{l_k} \in \mathbb{R}^{N\times N}$ in (22) realizes the reset action (1) on the components of $\hat{\mathbf{u}}$ related to the new leader l_k. This is a diagonal matrix having all zeros on the main diagonal except for the l_kth entry, which is set to one to ensure $\hat{\mathbf{u}}_{l_k}(t_k) = \mathbf{u}_r(t_k)$. Its complement is defined as $\mathbf{S}_{l_k} = \mathbf{I}_N - \bar{\mathbf{S}}_{l_k}$.

Recalling that $\mathbf{u}_r(t)$ is constant in $[t_k, t_{k+1})$, the dynamics of the error vector $\mathbf{e}(t) = [\mathbf{e}_\mathbf{p}^\top(t)\ \mathbf{e}_\mathbf{v}^\top(t)\ \mathbf{e}_{\hat{\mathbf{u}}}^\top(t)]^\top$ in this interval is correctly described by system (13). Using (22)–(24), we can derive the initial conditions $\mathbf{e}(t_k)$ as a function of the chosen leader l_k and of the received external command $\mathbf{u}_r(t_k)$

$$\mathbf{e}_\mathbf{p}(t_k) = (\mathbf{S}_{l_k}\otimes\mathbf{I}_d)\left((\mathbf{p}(t_k^-) - \mathbf{d}) - \mathbf{1}\otimes(\mathbf{p}_{l_k}(t_k^-) - \mathbf{d}_{l_k})\right) \tag{25}$$

$$\mathbf{e}_\mathbf{v}(t_k) = (\mathbf{S}_{l_k}\otimes\mathbf{I}_d)(\mathbf{v}(t_k^-) - \mathbf{1}\otimes\mathbf{v}_{l_k}(t_k^-)) \tag{26}$$

$$\mathbf{e}_{\hat{\mathbf{u}}}(t_k) = (\mathbf{S}_{l_k}\otimes\mathbf{I}_d)(\hat{\mathbf{u}}(t_k^-) - \mathbf{1}\otimes\mathbf{u}_r(t_k)). \tag{27}$$

From (25)–(27), it is straightforward to see that the choice of the leader l_k directly affects $\mathbf{e}(t_k)$. For this reason, whenever appropriate, we will use the notation $\mathbf{e}(t_k,\, l_k)$ to explicitly indicate this (important) dependency.

In order to define a valid metric for the error vector, we first state the following result which holds for any positive semidefinite matrix and then we provide a lemma that is preliminary to the main result of the section.

Proposition 2: Consider the Laplacian matrix $\mathbf{L} \in \mathbb{R}^{N\times N}$ of any connected graph with N vertexes and denote by λ_N the largest eigenvalue of $\mathbf{L}$. Assuming three constants $k_{n_1}, k_{n_2}, k_{n_3} \in \mathbb{R}$ such that

$$k_{n_1} > 0,\ k_{n_3} > 0 \ \text{ and } \ 0 < k_{n_2} < k_{n_1}/\sqrt{\lambda_N} \tag{28}$$

the matrix

$$\mathbf{P}_L := \begin{bmatrix} k_{n_1}\mathbf{G} + k_{n_3}\mathbf{I}_{dN} & k_{n_2}\mathbf{G} & \mathbf{0} \\ k_{n_2}\mathbf{G} & k_{n_1}\mathbf{I}_{dN} & \mathbf{0} \\ \mathbf{0} & \mathbf{0} & \mathbf{I}_{dN} \end{bmatrix} \in \mathbb{R}^{3dN\times 3dN} \tag{29}$$

where $\mathbf{G} = (\mathbf{L}\otimes\mathbf{I}_d) \in \mathbb{R}^{dN\times dN}$ is positive definite.

Proof: In order to prove the statement, it is sufficient to show that the eigenvalues of the symmetric matrix

$$\mathbf{P}^\star = \begin{bmatrix} k_{n_1}\mathbf{L} + k_{n_3}\mathbf{I}_N & k_{n_2}\mathbf{L} \\ k_{n_2}\mathbf{L} & k_{n_1}\mathbf{I}_N \end{bmatrix} \in \mathbb{R}^{2N\times 2N} \tag{30}$$

are all positive. Any eigenvalue μ_j, $j \in \{1,\dots,2N\}$ of $\mathbf{P}^\star$ must satisfy the relation $\mathbf{P}^\star\mathbf{v}_j = \mu_j\mathbf{v}_j$, where $\mathbf{v}_j \in \mathbb{R}^{2N}$ is the eigenvector associated with μ_j. If we left-multiply both sides of the previous relation with $(\boldsymbol{w}_i^\top \otimes \mathbf{I}_2) \in \mathbb{R}^{2\times 2N}$, where $\boldsymbol{w}_i \in \mathbb{R}^N$ is the left-eigenvector of $\mathbf{L}$ associated with the generic eigenvalue λ_i, $i \in \{1,\dots,N\}$, we obtain

$$\underbrace{\begin{bmatrix} k_{n_1}\lambda_i + k_{n_3} & k_{n_2}\lambda_i \\ k_{n_2}\lambda_i & k_{n_1} \end{bmatrix}}_{\mathbf{P}^\star_{\lambda_i}} \begin{bmatrix} \boldsymbol{w}_i^\top\mathbf{v}_{j,1} \\ \boldsymbol{w}_i^\top\mathbf{v}_{j,2} \end{bmatrix} = \mu_j \begin{bmatrix} \boldsymbol{w}_i^\top\mathbf{v}_{j,1} \\ \boldsymbol{w}_i^\top\mathbf{v}_{j,2} \end{bmatrix} \tag{31}$$

with $\mathbf{v}_j = [\mathbf{v}_{j,1}^\top\ \mathbf{v}_{j,2}^\top]^\top$. This, in turn, implies that μ_j must be an eigenvalue of the 2×2 matrix $\mathbf{P}^\star_{\lambda_i}$ for every $\lambda_i \in \sigma(\mathbf{L})$. Analytically computing the eigenvalues of $\mathbf{P}^\star_{\lambda_i}$ by solving a

quadratic equation, we obtain

$$\mu_j = \frac{1}{2}\left(k_{n_1}(\lambda_i+1)+k_{n_3}-\sqrt{\Delta}\right) \tag{32}$$

$$\mu_{2j} = \frac{1}{2}\left(k_{n_1}(\lambda_i+1)+k_{n_3}+\sqrt{\Delta}\right) \tag{33}$$

where

$$\Delta = (k_{n_1}(\lambda_i-1)+k_{n_3})^2 + 4k_{n_2}^2\lambda_i^2. \tag{34}$$

By then imposing $\mu_j, \mu_{2j} > 0$, we obtain

$$\lambda_i^2 k_{n_2}^2 < k_{n_1}^2\lambda_i + k_{n_3}k_{n_1} \tag{35}$$

which is always verified for $\lambda_i = 0$. For any other $\lambda_i > 0$, inequality (35) can be met by adopting the more restrictive constraint $\lambda_i^2 k_{n_2}^2 < k_{n_1}^2\lambda_i$, that is, $k_{n_2} < k_{n_1}/\sqrt{\lambda_i}$. The proof is concluded by noticing that the last inequality holds for every $\lambda_i \in \sigma(\mathbf{L})$ when k_{n_2} is set according to (28). ■

Lemma 1: Consider a positive definite symmetric matrix $\mathbf{A} \in \mathbb{R}^{N\times N}$ and denote by $0 < \phi_1 \leq, \ldots, \leq \phi_N$ its eigenvalues. Define the symmetric matrix

$$\mathbf{Q} := \mathrm{sym}\left(\mathbf{Q}_1\mathbf{Q}_2\right) = \frac{1}{2}\left(\mathbf{Q}_1\mathbf{Q}_2 + \mathbf{Q}_2^\top\mathbf{Q}_1^\top\right), \text{with} \tag{36}$$

$$\mathbf{Q}_1 = \begin{bmatrix} k_{n_1}\mathbf{A}+k_{n_3}\mathbf{I}_M & k_{n_2}\mathbf{A} & \mathbf{0} \\ k_{n_2}\mathbf{A} & k_{n_1}\mathbf{I}_M & \mathbf{0} \\ \mathbf{0} & \mathbf{0} & \mathbf{I}_M \end{bmatrix} \tag{37}$$

$$\mathbf{Q}_2 = \begin{bmatrix} \mathbf{0} & \mathbf{I}_M & \mathbf{0} \\ -\mathbf{A} & -b\mathbf{I}_M & b\mathbf{I}_M \\ \mathbf{0} & \mathbf{0} & -\mathbf{A} \end{bmatrix} \tag{38}$$

where $b, k_{n_1}, k_{n_2}, k_{n_3} > 0$, and $k_{n_2} < k_{n_1}/\sqrt{\phi_N}$ (to ensure the positive definiteness of $\mathbf{Q}_1$, according to Property 2).

If the following conditions are also met:

$$b < \phi_1 \tag{39}$$

$$k_{n_1} < \frac{2\phi_1}{b} \tag{40}$$

$$k_{n_2} < \min\left\{\frac{bk_{n_1}}{\phi_N(2+b)}, \frac{2}{b} - \frac{k_{n_1}}{\phi_1}\right\} \tag{41}$$

$$k_{n_3} < \frac{bk_{n_2}\phi_1}{2} \tag{42}$$

then the $3N$ eigenvalues of $\mathbf{Q}$ are all negative and, in particular, they are upper-bounded by the maximum between the following negative quantities

$$k_{n_2}\phi_1(b-\phi_1) \tag{43}$$

$$k_{n_2}\phi_N\left(1+\frac{b}{2}\right) - \frac{b}{2}k_{n_1} \tag{44}$$

$$\phi_1\left(\frac{b}{2}k_{n_2}-1\right) + \frac{b}{2}k_{n_1}. \tag{45}$$

Proof: After suitable computations, we obtain

$$\mathbf{Q} = \begin{bmatrix} -k_{n_2}\mathbf{A}^2 & -\frac{b}{2}k_{n_2}\mathbf{A}+k_{n_3}\mathbf{I}_M & \frac{b}{2}k_{n_2}\mathbf{A} \\ * & k_{n_2}\mathbf{A}-bk_{n_1}\mathbf{I}_M & \frac{b}{2}k_{n_1}\mathbf{I}_M \\ * & * & -\mathbf{A} \end{bmatrix}.$$

Any eigenvalue ν_j, $j \in \{1,\ldots,3N\}$ of $\mathbf{Q}$ must satisfy the relation $\mathbf{Q}\mathbf{v}_j = \nu_j\mathbf{v}_j$, where $\mathbf{v}_j \in \mathbb{R}^{3N}$ is the eigenvector related to ν_j. Left-multiplying both sides of the previous relation by $(\mathbf{I}_3 \otimes \boldsymbol{w}_i^\top) \in \mathbb{R}^{3\times 3N}$, where $\boldsymbol{w}_i \in \mathbb{R}^N$ is the left-eigenvector of $\mathbf{A}$ associated with the eigenvalue ϕ_i, $i \in \{1,\ldots,N\}$, we get

$$\begin{bmatrix} -k_{n_2}\phi_i^2 & -\frac{b}{2}k_{n_2}\phi_i + k_{n_3} & \frac{b}{2}k_{n_2}\phi_i \\ * & k_{n_2}\phi_i - bk_{n_1} & \frac{b}{2}k_{n_1} \\ * & * & -\phi_i \end{bmatrix} \begin{bmatrix} \boldsymbol{w}_i^\top\mathbf{v}_{j,1} \\ \boldsymbol{w}_i^\top\mathbf{v}_{j,2} \\ \boldsymbol{w}_i^\top\mathbf{v}_{j,3} \end{bmatrix}$$

$$= \nu_j \begin{bmatrix} \boldsymbol{w}_i^\top\mathbf{v}_{j,1} \\ \boldsymbol{w}_i^\top\mathbf{v}_{j,2} \\ \boldsymbol{w}_i^\top\mathbf{v}_{j,3} \end{bmatrix}$$

where $\mathbf{v}_j = [\mathbf{v}_{j,1}^\top\ \mathbf{v}_{j,2}^\top\ \mathbf{v}_{j,3}^\top]^\top$. This means that for every eigenvalue ϕ_i of $\mathbf{A}$, ν_j must be an eigenvalue of the 3×3 matrix

$$\mathbf{Q}_{\phi_i} = \begin{bmatrix} -k_{n_2}\phi_i^2 & -\frac{b}{2}k_{n_2}\phi_i + k_{n_3} & \frac{b}{2}k_{n_2}\phi_i \\ * & k_{n_2}\phi_i - bk_{n_1} & \frac{b}{2}k_{n_1} \\ * & * & -\phi_i \end{bmatrix}.$$

Applying the Gershgorin circle theorem, we know that every eigenvalue of $\mathbf{Q}_{\phi_i}$ is at least in one of the six disks (in the complex plane) centered on the three main diagonal terms of the matrix, and with the radius the sum of the magnitudes of the off-diagonal entries in same column or in the same row. Due to the symmetry of $\mathbf{Q}_{\phi_i}$ in our case, we have only three disks whose largest intersection with the real axis are, respectively

$$z_{i,1} := -k_{n_2}\phi_i^2 + \left|\tfrac{b}{2}k_{n_2}\phi_i - k_{n_3}\right| + \left|\tfrac{b}{2}k_{n_2}\phi_i\right|$$

$$z_{i,2} := k_{n_2}\phi_i - bk_{n_1} + \left|\tfrac{b}{2}k_{n_2}\phi_i - k_{n_3}\right| + \left|\tfrac{b}{2}k_{n_1}\right|$$

$$z_{i,3} := -\phi_i + \left|\tfrac{b}{2}k_{n_2}\phi_i\right| + \left|\tfrac{b}{2}k_{n_1}\right|.$$

By using the fact that $k_{n_1}, k_{n_2}, k_{n_3}, \phi_i$, and b are positive quantities and k_{n_3} also satisfies (42), we obtain

$$z_{i,1} < -k_{n_2}\phi_i^2 + bk_{n_2}\phi_i =: \bar{z}_{i,1} \tag{46}$$

$$z_{i,2} < k_{n_2}\phi_i\left(1+\tfrac{b}{2}\right) - \tfrac{b}{2}k_{n_1} =: \bar{z}_{i,2} \tag{47}$$

$$z_{i,3} = -\phi_i + \tfrac{b}{2}k_{n_2}\phi_i + \tfrac{b}{2}k_{n_1}. \tag{48}$$

Our goal is then to find the additional conditions on k_{n_1}, k_{n_2}, and k_{n_3} such that $\bar{z}_{i,1}, \bar{z}_{i,2}$, and $z_{i,3}$ are all negative for each $i \in \{1,\ldots,N\}$. Posing $\bar{z}_{i,1} < 0$ results in $b < \phi_i$, which is then equivalent to (39). Condition $\bar{z}_{i,2} < 0$ can be guaranteed if $k_{n_2} < \frac{b}{\phi_i(2+b)}k_{n_1}$, that is, it is equivalent to $k_{n_2} < \frac{b}{\phi_N(2+b)}k_{n_1}$. Condition $z_{i,3} < 0$ results in $k_{n_2} < \frac{2}{b} - \frac{k_{n_1}}{\phi_i}$, that is, $k_{n_2} < \frac{2}{b} - \frac{k_{n_1}}{\phi_1}$. Since it must be also $k_{n_2} > 0$, the last inequality can only be verified if $\frac{2}{b} - \frac{k_{n_1}}{\phi_1} > 0$, that is, if (40) holds. Condition (41) is the combination of the just mentioned upper-bounds on k_{n_2}, namely, it has to be simultaneously guaranteed that $k_{n_2} < \frac{b}{\phi_N(2+b)}k_{n_1}$ and $k_{n_2} < \frac{2}{b} - \frac{k_{n_1}}{\phi_1}$. Finally, the values in (43)–(45) represent the values of $\bar{z}_{i,1}$, $\bar{z}_{i,2}$, and $z_{i,3}$, respectively, where ϕ_i has always been chosen as the worst case according to the assumption that $0 < \phi_1 \leq, \ldots, \leq \phi_N$. ■

The following result finally gives an explicit characterization of the behavior of $\mathbf{e}(t)$ during the interval $[t_k, t_{k+1})$, which then naturally leads to the subsequent definition of optimal leader

selection. For the sake of exposition, we assume that $k_p = k_u = 1$. All of the results easily extend to the more general case $k_p > 0, k_u > 0$ with more tedious machinery.

Proposition 3: Consider the error vector $\mathbf{e}(t)$ with a specific leader l_k and, w.l.o.g., $k_p = k_u = 1$. If the constants $b, k_{n_1}, k_{n_2}, k_{n_3}$ are chosen in order to satisfy the next conditions

$$0 < b < \lambda_{2,l_k},\ 0 < k_{n_1} < \frac{2\lambda_{2,l_k}}{b},\ 0 < k_{n_3} < \frac{bk_{n_2}\lambda_{2,l_k}}{2}$$
$$0 < k_{n_2} < \min\left\{\frac{bk_{n_1}}{\lambda_{N,l_k}(2+b)}, \frac{2}{b} - \frac{k_{n_1}}{\lambda_{2,l_k}}, \frac{k_{n_1}}{\sqrt{\lambda_{N,l_k}}}\right\} \tag{49}$$

then the error metric $\|\mathbf{e}(t)\|_L^2 := \mathbf{e}^\top(t)\mathbf{P}_L\mathbf{e}(t)$ is monotonically decreasing in the time interval $[t_k, t_{k+1})$ wherein the topology is assumed to be fixed. In particular, the error metric behavior is dominated by the following exponential upper bound:

$$\|\mathbf{e}(t)\|_L^2 \le \|\mathbf{e}(t_k)\|_L^2\, e^{-2\,\nu_{l_k}(t-t_k)} \quad \forall t \in [t_k, t_{k+1}) \tag{50}$$

where $\nu_{l_k} > 0$ is the minimum among the following quantities:

$$\nu_{l_k} = \min\begin{cases} k_{n_2}\lambda_{2,l}(\lambda_{2,l} - b) \\ \frac{b}{2}k_{n_1} - k_{n_2}\lambda_{N,l}\left(1 + \frac{b}{2}\right) \\ \lambda_{2,l} - \frac{b}{2}(k_{n_2}\lambda_{2,l} + k_{n_1}). \end{cases} \tag{51}$$

Proof: The dynamics of the error $\mathbf{e}(t)$ in $[t_k, t_{k+1})$, with $k_p = k_u = 1$ reduces to

$$\begin{bmatrix}\dot{\mathbf{e}}_\mathbf{p} \\ \dot{\mathbf{e}}_\mathbf{v} \\ \dot{\mathbf{e}}_{\hat{\mathbf{u}}}\end{bmatrix} = \begin{bmatrix}\mathbf{0} & \mathbf{I}_{dN} & \mathbf{0} \\ \mathbf{G}_l & -b\mathbf{I}_{dN} & b\mathbf{I}_{dN} \\ \mathbf{0} & \mathbf{0} & \mathbf{G}_l\end{bmatrix}\begin{bmatrix}\mathbf{e}_\mathbf{p} \\ \mathbf{e}_\mathbf{v} \\ \mathbf{e}_{\hat{\mathbf{u}}}\end{bmatrix} \tag{52}$$

where we omit (as in the following) the time dependency for the sake of exposition. The subvectors $\mathbf{e}_{\mathbf{p},l}$, $\mathbf{e}_{\mathbf{v},l}$, and $\mathbf{e}_{\hat{\mathbf{u}},l}$ are zero at $t = t_k$ and their dynamics is invariant, due to the row of zeros in $\mathbf{L}_l$ corresponding to the agent l, i.e.,

$$\mathbf{e}_{\mathbf{p},l} = \mathbf{e}_{\mathbf{v},l} = \mathbf{e}_{\hat{\mathbf{u}},l} = \dot{\mathbf{e}}_{\mathbf{p},l} = \dot{\mathbf{e}}_{\mathbf{v},l} = \dot{\mathbf{e}}_{\hat{\mathbf{u}},l} = \mathbf{0} \quad \forall t \in [t_k, t_{k+1}).$$

Hence, we can restrict our analysis to the dynamics of the orthogonal subspace, that is, of the remaining components $\mathbf{e}_{\mathbf{p},i}$, $\mathbf{e}_{\mathbf{v},i}$, and $\mathbf{e}_{\hat{\mathbf{u}},i}, \forall i \ne l$. We denote by ${}^l\mathbf{e}_\mathbf{p}$, ${}^l\mathbf{e}_\mathbf{v}$, and ${}^l\mathbf{e}_{\hat{\mathbf{u}}}$ the $d(N-1)$-vectors obtained by removing the d entries corresponding to l in $\mathbf{e}_\mathbf{p}$, $\mathbf{e}_\mathbf{v}$, and $\mathbf{e}_{\hat{\mathbf{u}}}$, respectively, and with ${}^l\mathbf{e}$ their concatenation. Therefore, we have

$${}^l\dot{\mathbf{e}} = \begin{bmatrix}{}^l\dot{\mathbf{e}}_\mathbf{p} \\ {}^l\dot{\mathbf{e}}_\mathbf{v} \\ {}^l\dot{\mathbf{e}}_{\hat{\mathbf{u}}}\end{bmatrix} = \begin{bmatrix}\mathbf{0} & \mathbf{I}_{(N-1)d} & \mathbf{0} \\ {}^l\mathbf{G}_l & -b\mathbf{I}_{(N-1)d} & b\mathbf{I}_{(N-1)d} \\ \mathbf{0} & \mathbf{0} & {}^l\mathbf{G}_l\end{bmatrix}{}^l\mathbf{e} = \mathbf{D}_l{}^l\mathbf{e} \tag{53}$$

where ${}^l\mathbf{G}_l = -(\mathbf{M}_l \otimes \mathbf{I}_d) \in \mathbb{R}^{(N-1)d\times(N-1)d}$.

We now consider the error metric dynamics. First, note that

$$\|\mathbf{e}\|_L^2 = \mathbf{e}^\top\mathbf{P}_L\mathbf{e} = {}^l\mathbf{e}^\top\mathbf{P}_{M_l}{}^l\mathbf{e} = \|{}^l\mathbf{e}\|_{M_l}^2 \tag{54}$$

where $\mathbf{P}_{M_l} \in \mathbb{R}^{3d(N-1)\times 3d(N-1)}$ is defined as (29) with ${}^l\mathbf{G}_l$ and $\mathbf{I}_{d(N-1)}$ in place of $\mathbf{G}$ and $\mathbf{I}_{dN}$, respectively. Notice that the positive definiteness of $\mathbf{P}_L$ implies that also $\mathbf{P}_{M_l}$ is a positive definite matrix for all l; thus, the metrics $\|{}^l\mathbf{e}\|_{M_l}^2$ are well defined for all l according to Property 3. Hence, we have

$$\begin{aligned}\frac{d}{dt}\|\mathbf{e}\|_L^2 &= \frac{d}{dt}\|{}^l\mathbf{e}\|_{M_l}^2 \\ &= 2{}^l\mathbf{e}^\top\mathbf{P}_{M_l}{}^l\dot{\mathbf{e}} = 2{}^l\mathbf{e}^\top\mathbf{P}_{M_l}\mathbf{D}_l{}^l\mathbf{e} \\ &= 2{}^l\mathbf{e}^\top\mathrm{sym}(\mathbf{P}_{M_l}\mathbf{D}_l){}^l\mathbf{e} \le 2\mu_{\max,l}\|{}^l\mathbf{e}\|_{M_l}^2\end{aligned} \tag{55}$$

where $\mu_{\max,l}$ is the largest eigenvalue of the symmetric part of $\mathbf{P}_{M_l}\mathbf{D}_l$. Accounting for equality (54), (55) implies that for all $t \in [t_k, t_{k+1})$, it holds that

$$\|\mathbf{e}(t)\|_L^2 \le \|\mathbf{e}(t_k)\|_L^2\, e^{2\,\mu_{\max,l_k}(t-t_k)} \tag{56}$$

which coincides with (50) proving that $\mu_{\max,l} = -\nu_l$, where ν_l is defined as in the proposition.

To this and first of all we note that due to the properties of the Kronecker product, the eigenstructure of $\mathrm{sym}(\mathbf{P}_{M_L}\mathbf{D}_l)$ is obtained by repeating d times the structure of matrix $\mathbf{Q}$ in (36) by choosing $\mathbf{A} = \mathbf{M}_l$. Applying Lemma 1 with $\mathbf{A} = \mathbf{M}_l$ and, thus, $\phi_1 = \lambda_{2,l}$ and $\phi_N = \lambda_{N,l}$, we obtain that if $k_{n_1}, k_{n_2}, k_{n_3}$ are chosen as in the assumption of the proposition, then $-\nu_l$ is the maximum eigenvalue of $\mathbf{Q}$ which results upper-bounded by the maximum of the quantities in Lemma 1. This, in turn, yields a lower-bound for ν_l by the minimum among the quantities in the proposition. ■

For the reader's convenience, we report in Fig. 1 the values of $\lambda_{2,l}$ versus λ_2 and of $\lambda_{N,l}$ versus λ_N for different leaders l and across different graph topologies.

Thanks to the upper bound (50) at every instant $t = t_k$, it is possible to estimate the maximum future decrease of the error vector $\mathbf{e}(t)$ in the interval $[t_k, t_{k+1})$. By evaluating (50) at $t = t_{k+1}^-$, that is, just before the next leader selection, we obtain

$$\|\mathbf{e}(t_{k+1}^-)\|_L^2 \le \|\mathbf{e}(t_k,\, l_k)\|_L^2\, e^{-2\,\nu_{l_k}T}. \tag{57}$$

Note that both $\mathbf{e}(t_k,\, l_k)$ and ν_{l_k} depend on the value of the current leader l_k. As a consequence, the right-hand side of (57) can be exploited for choosing the leader at time t_k in order to maximize the convergence rate of $\mathbf{e}(t)$ during the interval $[t_k, t_{k+1})$ and, therefore, improving at the same time both the tracking of the reference velocity and of the desired formation.

These observations are gathered in the following Fact.

Fact 1: Consider an N-agent system required to accomplish the dual task modeled in Section II according to the leader–follower paradigm. Within the online leader selection context, in order to improve the tracking performance of the reference velocity and of the desired formation during the interval $[t_k,\, t_{k+1})$ having duration T, the leader should be selected so that it solves the following minimization problem:

$$\arg\min_{l\in\mathcal{L}_k} f_k(l), \quad \text{with} \quad f_k(l) = \|\mathbf{e}(t_k,\, l_k)\|_L^2\, e^{-2\,\nu_l T} \tag{58}$$

where $\mathcal{L}_k \subseteq \{1, \ldots, N\}$ is the set of "eligible" agents from which a leader can be selected at t_k and the error metric defined in Property 3 is used.

In Fact 1, the concept of "eligible" agents is introduced for the first time; however, this will be clarified in the following

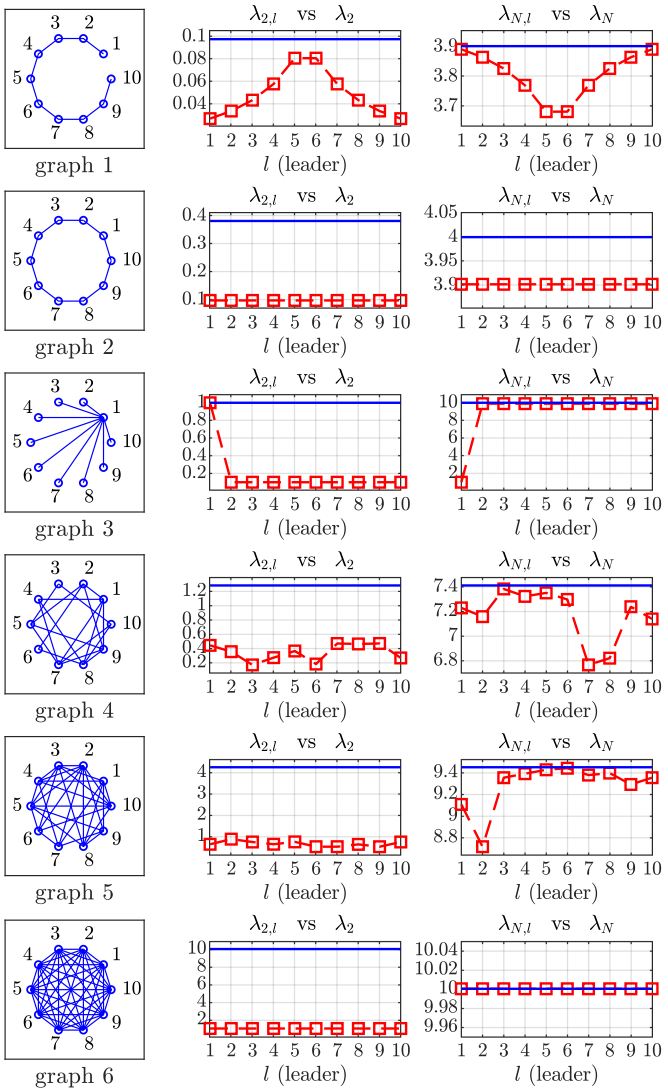

Fig. 1. Values of $\lambda_{2,l}$ versus λ_2 and $\lambda_{N,l}$ versus λ_N for different leaders l. The squares correspond to values of $\lambda_{2,l}$ and $\lambda_{N,l}$ associated with a leader $l = 1, \ldots, N$, with $N = 10$. The solid constant blue lines represent λ_2 and λ_N. Each row corresponds to a different graph with $N = 10$ vertexes. From top to bottom: the line, ring, star, two random (connected) graphs, and a clique graph.

section. In the following text, we highlight two crucial aspects related to the minimization problem (58).

Remark 1: Similar to the first-order case, the minimization problem (58) needs to be solved *online* because of the dependency of the cost function on both the group topology and the current multiagents system state.

Remark 2: The reset action (1) implies the zeroing of the components of the estimation error vector $\mathbf{e}_{\hat{u}}$ associated with the current leader l_k. Hence, the quantity $\|\mathbf{e}(t_k, l_k)\|_L^2$ may decrease at every instance of the leader selection. Thus, it would be desirable to reduce the leader selection period T as much as possible. However, in practice, there exists a *maximum frequency* at which the leader selection process can be executed, guaranteeing the successful procedure termination under real-world constraints. This entails the existence of a finite minimum selection period $T_{\min}$ such that $T \geq T_{\min} > 0$.

IV. Distributed Next Best Leader Selection

The contribution of this section is a fully distributed procedure to solve the optimization problem (58). To cope with the distributiveness requirement, the set of agents eligible as leader, namely, the set $\mathcal{L}_k$ introduced in Fact 1, is restricted to the neighborhood of the *current* leader, that is, $\mathcal{L}_k = \mathcal{N}_{l_k}$. As better explained in the following text, this choice ensures the possibility of each agent belonging to $\mathcal{L}_k$ to evaluate the quantity $f_k(l)$ in (58) (depending on the current leader) through a local information exchange. Nevertheless, this also implies that the minimization (58) is performed only locally, that is, in $\mathcal{L}_k = \mathcal{N}_{l_k}$, thus, the achieved minimum might not be global. To guarantee a global optimum, indeed, $f_k(l)$ should be minimized over all agents in the group, that is, setting $\mathcal{L}_k = \{1, \ldots, N\}$. However, this would result in fully centralized optimization whenever $\mathcal{G}$ is not the complete graph since it entails that all agents have global knowledge of the network. In our method, the global optimum is instead approximated by the repetition, at every time T, of the minimization (58) in the neighborhood of the current leader. In this way, the computation load is spread among the agents and over time, as is customary in distributed approaches. We shall see in Section V that this choice is a good compromise between distributiveness and global optimality.

We now consider the evaluation of the cost function $f_k(m)$ in (58) by any leader-candidate $m \in \mathcal{N}_{l_k}$. This requires the knowledge of the error norm $\|\mathbf{e}(t_k, m)\|_L^2$ and of the eigenvalues $\lambda_{2,m}$ and $\lambda_{N,m}$ in order to compute ν_m through (51). Although all of them are global quantities, in the following text we will prove that they can be locally retrieved by restoring some well-known distributed estimation techniques.

First, for any $m \in \mathcal{N}_{l_k}$ both $\lambda_{2,m}$ and $\lambda_{N,m}$ can be locally estimated exploiting a simplified version of the *Decentralized Power Iteration algorithm* proposed in [26] and based on the PI average consensus estimating (*PI-ace*) technique introduced in [27]. Thanks to the consensus-based mechanism, the PI-ace strategy allows the mth agent belonging to the group $\mathcal{N}_{l_k}$ to build a local estimation $\hat{\boldsymbol{w}}_k$ of the eigenvector $\boldsymbol{w}_k$ of $\mathbf{M}_m$ corresponding to the eigenvalue $\lambda_{k,m}$, $k \in \{2, N\}$. In this way, the estimate $\hat{\lambda}_{k,m} = -(\sum_{n \in \mathcal{N}_m} [\mathbf{M}_m]_{m,n} [\hat{\boldsymbol{w}}_k]_n)[\hat{\boldsymbol{w}}_k]_m^{-1}$ can be derived by employing only locally available information. The convergence of such a procedure is ensured by a suitable choice of the eigenvector estimation gains and initial conditions as discussed in [26] and [27].

Also, the error norm $\|\mathbf{e}(t_k, m)\|_L^2$ can be estimated by any leader-candidate $m \in \mathcal{N}_{l_k}$ via a distributed procedure requiring information locally available and recoverable via 1-hop communication (i.e., directly provided by a neighboring node). To prove this fact, omitting all dependencies for the sake of brevity, we rewrite the scalar quantity $\|\mathbf{e}(t_k, m)\|_L^2$ as

$$\begin{aligned}\mathbf{e}^\top \mathbf{P}_L \mathbf{e} = {} & k_{n_3} \mathbf{e}_{\mathbf{p}}^\top \mathbf{e}_{\mathbf{p}} + k_{n_1} \mathbf{e}_{\mathbf{v}}^\top \mathbf{e}_{\mathbf{v}} + \mathbf{e}_{\hat{\mathbf{u}}}^\top \mathbf{e}_{\hat{\mathbf{u}}} \\ & + k_{n_1} \mathbf{e}_{\mathbf{p}}^\top \mathbf{G} \mathbf{e}_{\mathbf{p}} + 2 k_{n_2} \mathbf{e}_{\mathbf{p}}^\top \mathbf{G} \mathbf{e}_{\mathbf{v}} \end{aligned} \tag{59}$$

and we note that $\|(\mathbf{S}_m \otimes \mathbf{I}_d)\boldsymbol{x}\|^2 = \sum_{i=1}^N \|\boldsymbol{x}_i\|^2 - \|\boldsymbol{x}_m\|^2$. As a consequence, by recalling (25)–(27) and denoting with the superscript $^-$ that all quantities computed at t_k^- and with $\tilde{\mathbf{p}}^-$

and the difference $\mathbf{p}^- - \mathbf{d}$, the first three terms in (59) can be rewritten accounting for the following identities:

$$\begin{aligned}\mathbf{e}_\mathbf{p}^\top \mathbf{e}_\mathbf{p} &= \sum_{i=1}^{N} \|\tilde{\mathbf{p}}_i^- - \tilde{\mathbf{p}}_m^-\|^2 + 0 \\ &= \sum_{i=1}^{N} \tilde{\mathbf{p}}_i^{-\top} \tilde{\mathbf{p}}_i^- - 2\tilde{\mathbf{p}}_m^{-T} \sum_{i=1}^{N} \tilde{\mathbf{p}}_i^- + N \tilde{\mathbf{p}}_m^{-\top} \tilde{\mathbf{p}}_m^- \end{aligned} \tag{60}$$

$$\begin{aligned}\mathbf{e}_\mathbf{v}^\top \mathbf{e}_\mathbf{v} &= \sum_{i=1}^{N} \|\mathbf{v}_i^- - \mathbf{v}_m^-\|^2 + 0 \\ &= \sum_{i=1}^{N} \mathbf{v}_i^{-\top} \mathbf{v}_i^- + 2\mathbf{v}_m^{-\top} \sum_{i=1}^{N} \mathbf{v}_i^- + N \mathbf{v}_m^{-\top} \mathbf{v}_m^- \end{aligned} \tag{61}$$

$$\begin{aligned}\mathbf{e}_{\hat{\mathbf{u}}}^\top \mathbf{e}_{\hat{\mathbf{u}}} &= \sum_{i=1}^{N} \|\hat{\mathbf{u}}_i^- - \mathbf{u}_r\|^2 - \|\hat{\mathbf{u}}_m^- - \mathbf{u}_r\|^2 \\ &= \sum_{i=1}^{N} \hat{\mathbf{u}}_i^{-\top} \hat{\mathbf{u}}_i^- - 2\mathbf{u}_r^\top \sum_{i=1}^{N} \hat{\mathbf{u}}_i^- + N \mathbf{u}_r^\top \mathbf{u}_r - \|\hat{\mathbf{u}}_m^- - \mathbf{u}_r\|^2. \end{aligned} \tag{62}$$

Therefore, the quantity $\|\mathbf{e}(t_k, m)\|_L^2$ can be evaluated by any agent $m \in \mathcal{N}_{l_k}$ as a function of:

1) the vectors $\mathbf{p}_m(t_k^-)$, $\mathbf{v}_m(t_k^-)$ and $\hat{\mathbf{u}}_m(t_k^-)$;
2) the vector $\mathbf{u}_r(t_k)$;
3) the three vectors $\sum_{i=1}^N \hat{\mathbf{u}}_i(t_k^-)$, $\sum_{i=1}^N \mathbf{v}_i(t_k^-)$, and $\sum_{i=1}^N (\mathbf{p}_i(t_k^-) - \mathbf{d}_i)$;
4) the three scalar quantities $\sum_{i=1}^N \hat{\mathbf{u}}_i^{-\top} \hat{\mathbf{u}}_i^-$, $\sum_{i=1}^N \mathbf{v}_i^{-\top} \mathbf{v}_i^-$, and $\sum_{i=1}^N \tilde{\mathbf{p}}_i^{-\top} \tilde{\mathbf{p}}_i^-$;
5) the total number of agents N.

The vectors listed in 1) are locally available to agent m and, similarly, $\mathbf{u}_r(t_k)$ is locally available to agent m via 1-hop communication from the current leader l_k. On the other hand, the quantities listed in 3) and 4) can be locally estimated by employing the PI-ace strategy mentioned before. Finally, the total number of agents N can be assumed to be an *a priori* information locally available to each agent; otherwise, one can resort to an additional distributed scheme (see, e.g., [28]) to obtain its value over time. This analysis thus proves that any agent $m \in \mathcal{N}_{l_k}$ can compute $\|\mathbf{e}(t_k, m)\|_L^2$ by exploiting only local and 1-hop communication information.

We have thus shown that all quantities involved in the evaluation of $f_k(m)$ in (58) can be locally achieved by any leader-candidate $m \in \mathcal{N}_k$. Hence, at every t_k, the optimal leader selection can be performed by the agents group in a distributed way according to the procedure summarized in Algorithm 1. This is hereafter referred to as Distributed and Optimized Online Leader Selection (*DO2 Leader Selection*). Note that its convergence is ensured by the convergence results on the decentralized power iteration method and the PI-ace scheme provided in [26] and [27], respectively.

V. Simulation Results

This section is devoted to the validation of the proposed DO2 Leader Selection approach through the comparison with other

Algorithm 1: *DO2 Leader Selection.*

Denote by l_0 the first selected leader
$k \leftarrow 0$
while *true* **do**
  agent l_k informs the reference source about its leadership
  agent l_k waits time T
  $k \leftarrow k + 1$
  if $kT/T_r \in \mathbb{N}$ **then**
    agent l_{k-1} receives a new value of $\mathbf{u}_r(t_k)$ from the reference source
  if *a new* $\mathbf{u}_r(t_k)$ *is received* **then**
    agent l_{k-1} sends $\mathbf{u}_r(t_k)$ to every neighbor in $\mathcal{N}_{k-1}$
  every agent $m \in \mathcal{N}_{l_{k-1}}$ sends $f_k(l)$ to agent l_{k-1}
  agent l_{k-1} computes the set $\mathcal{L}^* = \text{argmin}_{m \in \mathcal{L}_{k-1}} f_k(m)$
  if $l_{k-1} \in \mathcal{L}^*$ **then**
    $l_k = l_{k-1}$
  else
    agent l_{k-1} nominates l_k in $\mathcal{L}^*$, e.g., randomly

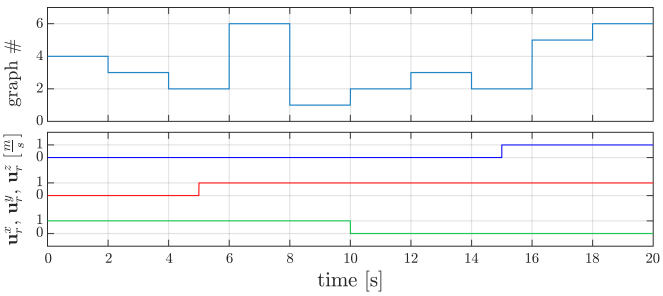

Fig. 2. Current graph $\mathcal{G}$ topology (top) and components of the external velocity reference $\mathbf{u}_r$ (bottom).

trivial although intuitive leader selection procedures. These consist of a *random* leader selection among all agents in the group and a *no* leader selection envisaging a constant (*a priori* chosen) leader during all of the task executions. To highlight the effectiveness of the DO2 Leader Selection strategy, we also consider its centralized version such that at each iteration, the leader is selected by setting $\mathcal{L}_k = \{1, \ldots, N\}$: this allows to evaluate the gap between the global optimal solution and the local one computed through Algorithm 1.

Numerical simulations are performed accounting for a group of $N = 10$ agents modeled as point masses in $\mathbb{R}^d$ with $d = 3$. All of the runs start from the same initial conditions on the agents position and assume time-varying agents interaction. In detail, the interaction graph $\mathcal{G}$ changes according to Fig. 2, which reports on the top of the topology variations with indexing defined in Fig. 1: we simulate the decrease of the connectivity level to show the robustness of the DO2 Leader Selection algorithm w.r.t. to the communication amount. The reference velocity $\mathbf{u}_r(t) \in \mathbb{R}^3$ is behaviored as a piece-wise constant function of period $T_r = 5$ s w.r.t. its three components as depicted on the bottom of Fig. 2. For the random and optimized strategies, the leader selection period is set to $T = 0.05$ s. Finally, the gains $k_p = 2$, $k_u = 1$, $b = 0.01$ are used in the network dynamics model and all of the PI-ace estimators are designed to converge to the consensus value in a finite number of iterations limiting the final estimation error.

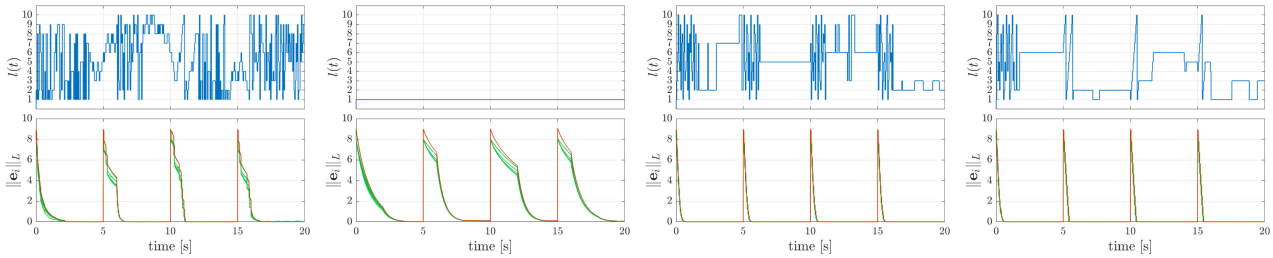

(a) random leader selection (b) no leader selection (c) globally optimized leader selection (d) locally optimized leader selection

Fig. 3. Identity of the current leader $l(t)$ (top) and error metric $\|\mathbf{e}_i(t)\|_L$ $i = 1, \ldots, N$ (bottom) by applying different leader selection strategies. (a) Random leader selection. (b) No leader selection. (c) Globally optimized leader selection. (d) Locally optimized leader selection.

TABLE I
LEADERSHIP CHANGES USING VARIOUS LEADER SELECTIONS

	leadership changes
random leader selection	288
no leader selection	0
globally optimized leader selection	130
locally optimized leader selection	85

The results of the simulations are shown in Fig. 3(a)–(d): the plots on the top depict the result of the leader selection procedure (i.e., the time-varying leader identity $l(t)$) and the plots on the bottom report the corresponding error norm $\|\mathbf{e}_i(t)\|_L$, $i = 1, \ldots, N$ defined by matrix $\mathbf{P}_L$ in (29) highlighting the value related to the current leader (orange line).

First, we can observe that the constant leader strategy [see Fig. 3(b)] presents the worst performance in minimizing $\|\mathbf{e}_i(t)\|_L$ w.r.t. the other cases, even though the convergence of the errors toward zero is achieved, in accordance with Property 3. Note that, w.l.o.g., we have assumed that the leader constantly coincides with agent 1. However, when a fixed topology is considered, the performance of the constant leader solution might improve by choosing the leader that optimizes the error convergence rate computing the value ν_l for each $l \in \{1, \ldots, 10\}$ according to (51) (see Fig. 1 for the values of $\lambda_{2,l}$ and $\lambda_{N,l}$). The random leader selection [see Fig. 3(a)] performs better than the constant leader strategy, but its convergence time is much worse w.r.t. the optimized (both globally and locally) leader selection cases in Fig. 3(c) and (d). Indeed, randomly picking the next leader among the neighbors of the current leader makes the error converge to zero in a time between 1 and 2 s, while adopting the local DO2 Leader Selection strategy, the convergence time is always below 0.5 s. In addition, the results of the local DO2 Leader Selection strategy in Fig. 3(d) concerning the error behavior are comparable to the ones of its global version in Fig. 3(c). This implies that the suboptimal solution derived from the use of a distributed paradigm approaches the global optimum provided by the centralized approach. Furthermore, the local DO2 Leader Selection strategy visually results in fewer leader identity changes (plots on the top). To clarify this point, Table I reports the number of leadership changes over the considered period for each leader selection strategy.

The following has to be noted: while the random strategy changes the leader almost at each iteration T, the DO2 Leader Selection strategy (especially the local version) tends to "stabilize" the leader choice as the error norm $\|\mathbf{e}_i(t)\|_L$ converges to zero, that is, when the tracking transient becomes negligible and the group of agents has reached a steady state in its tracking performance. This fact constitutes an important advantage of the DO2 Leader Selection strategy w.r.t. the random one since in real-world applications, the constant change of leadership would correspond to the need of continuously re-establishing new connections from the reference source side. Furthermore, from this point of view, to perform a local optimization is more advantageous than a global one.

VI. FIRST-ORDER VERSUS SECOND-ORDER CASE

In this section, we aim at figuring out the main differences between the first-order leader election addressed in [24] and the second-order case faced in this paper. The purpose is to highlight both the challenging aspects and the benefits derived from the employment of a more complex dynamic model for the multiagent group. These are listed as follows.

1) In [24], the described agents group is behaviored as a *first-order* system since the single-integrator model represents the simplest way to characterize a mobile agent dynamics. Here, we deal with *second-order* systems to describe the dynamics of a multiagent team. Despite the increased complexity, this choice is motivated by the fact that these systems better approximate the behavior of physical agentic agents and that controlling acceleration (rather than velocity) generally allows an agent to realize smooth movements.
2) Contrary to [24], in general, it occurs that $\mathbf{e_v} \neq \mathbf{v} - \mathbf{1} \otimes \mathbf{u}_r$. The leader velocity asymptotically converges to the reference $\mathbf{u}_r$ via (4); however, since the control acts at an acceleration level, one has that $\mathbf{v}_l \neq \mathbf{u}_r$ during any transient phase.
3) The initial condition $\hat{\mathbf{u}}(t_k)$ depends on the chosen leader l_k and is, in general, discontinuous at t_k. The position vector $\mathbf{p}(t)$ and (contrary to [24]) the velocity vector $\mathbf{v}(t)$ are instead continuous at t_k.
4) Property 3 proves that the scalar metric $\|\mathbf{e}(t)\|_L^2$ is monotonically decreasing along the system trajectories, while this is not guaranteed to hold for other metrics such as the

ℓ_2-norm $\|\mathbf{e}(t)\|^2$ as well as the one introduced in [24] for the first-order case. Hence, the definition of the matrix $\mathbf{P}_L$ and the results stated in Property 3 represent novel and original contributions of this paper, when compared with [24].

5) $\mathbf{P}_L$ is significantly more complex matrix than its first-order counterpart ($\mathbf{P}_{k_n}$ in [24]) and it is not at all a straightforward extension of it. $\mathbf{P}_{k_n}$ is basically a "scaled" identity matrix, while $\mathbf{P}_L$ contains several repetitions of the Laplacian matrix and is no longer a diagonal matrix. An important contribution of our work has been to find a matrix, such as $\mathbf{P}_L$, so that:
   a) can be made positive definite, so that it can represent a well-defined norm;
   b) makes the matrix $\mathbf{Q}$ positive definite as well, in order to define monotonically decreasing error dynamics;
   c) has a distributed structure, so that the error can be computed in a distributed way using distributed estimation.

   Finding such a matrix, with a structure completely different from the first-order case, is one of the main cornerstones of this paper.
6) We have shown that in the first-order leader election, only the knowledge of the smallest eigenvalue $\lambda_{2,m}$ of the matrix $\mathbf{M}_m$ is required. Considering a second-order dynamics, the value of the maximum eigenvalue $\lambda_{N,m}$ is required since the parameter ν_m depends on both quantities.
7) The structure of Algorithm 1 here proposed is similar to the one in [24]. The similarity is, however, limited since the computation of $f_k(m)$ (row 11) in the second-order cases is different from the first-order one. Furthermore, in the second-order case, this computation requires the estimation of three (instead of four as in the first-order case) scalar quantities because of the continuity of the velocity vector $\mathbf{v}$. This results in a simpler implementation compared to the first-order case since one less PI-ace filter is needed.

VII. Conclusion and Future Works

In this paper, we deal with the problem of *online leader selection* for a group of agents whose dynamics is modeled as a second-order system. The key idea is to treat the leader identity as a time-varying quantity to be chosen in order to optimize the performance in tracking an external velocity reference signal and in achieving a desired formation shape. For this goal, a suitable *tracking error metric* has been defined to capture the leadership changing effect in group performance.

A distributed leader selection procedure has then been proposed: during the agent motion, the DO2 Leader Selection algorithm aims at persistently selecting the best leader w.r.t. the defined tracking error metric. The validity of the proposed approach has been stated comparing the DO2 strategy with other more trivial solutions such as keeping a constant leader over time (as is typically done), or relying on a random choice.

As future developments, we want to extend our analysis by allowing the presence of multiple reference sources/leaders and accounting for other optimization criteria such as, for example, controllability.

References

[1] Y. Wang, E. Garcia, D. Casbeer, and F. Zhang, *Cooperative Control of Multi-Agent Systems: Theory and Applications*. Hoboken, NJ, USA: Wiley, 2017.

[2] R. Olfati-Saber, "Flocking for multi-agent dynamic systems: Algorithms and theory," *IEEE Trans. Autom. Control*, vol. 51, no. 3, pp. 401–420, Mar. 2006.

[3] W. Ren and R. W. Beard, *Distributed Consensus in Multi-Vehicle Cooperative Control: Theory and Applications*. Berlin, Germany: Springer, 2008.

[4] W. Ren and Y. Cao, *Distributed Coordination of Multi-Agent Networks: Emergent Problems, Models, and Issues*. Berlin, Germany: Springer, 2010.

[5] G. Notarstefano, M. Egerstedt, and M. Haque, "Containment in leader follower networks with switching communication topologies," *Automatica*, vol. 47, no. 5, pp. 1035–1040, 2011.

[6] Z. Meng, D. V. Dimarogonas, and K. H. Johansson, "Leader–follower coordinated tracking of multiple heterogeneous lagrange systems using continuous control," *IEEE Trans. Robot.*, vol. 30, no. 3, pp. 739–745, Jun. 2014.

[7] A. Loria, J. Dasdemir, and N. A. Jarquin, "Leader–follower formation and tracking control of mobile robots along straight paths," *IEEE Trans. Control Syst. Technol.*, vol. 24, no. 2, pp. 727–732, Mar. 2016.

[8] F. A. Yaghmaie, R. Su, F. L. Lewis, and L. Xie, "Multi-party consensus of linear heterogeneous multi-agent systems," *IEEE Trans. Autom. Control*, vol. 62, no. 11, pp. 5578–5589, Nov. 2017.

[9] G. Franzè, W. Lucia, and F. Tedesco, "A distributed model predictive control scheme for leader–follower multi-agent systems," *Int. J. Control*, vol. 91, pp. 369–382, 2017.

[10] H. Cai and G. Hu, "Distributed tracking control of an interconnected leader-follower multi-agent system," *IEEE Trans. Autom. Control*, vol. 62, no. 7, pp. 3494–3501, Jul. 2017.

[11] M. Tognon, C. Gabellieri, L. Pallottino, and A. Franchi, "Aerial comanipulation with cables: The role of internal force for equilibria, stability, and passivity," *IEEE Robot. Autom. Lett.*, vol. 3, no. 3, pp. 2577–2583, Jul. 2018.

[12] C. Gabellieri, M. Tognon, L. Palottino, and A. Franchi, "A study on force-based collaboration in flying swarms," in *Proc. 11th Int. Conf. Swarm Intell.*, Rome, Italy, Oct. 2018, pp. 3–15.

[13] S. Patterson and B. Bamieh, "Leader selection for optimal network coherence," in *Proc. 49th IEEE Conf. Decis. Control*, Atlanta, GA, USA, Dec. 2010, pp. 2692–2697.

[14] L. Vassio, F. Fagnani, P. Frasca, and A. Ozdaglar, "Message passing optimization of harmonic influence centrality," *IEEE Trans. Control Netw. Syst.*, vol. 1, no. 1, pp. 109–120, Mar. 2014.

[15] S. Pequito, V. Preciado, and G. J. Pappas, "Distributed leader selection," in *Proc. 54th IEEE Conf. Decis. Control*, Osaka, Japan, 2015, pp. 962–967.

[16] F. Lin, M. Fardad, and M. R. Jovanović, "Algorithms for leader selection in stochastically forced consensus networks," *IEEE Trans. Autom. Control*, vol. 59, no. 7, pp. 1789–1802, Jul. 2014.

[17] S. Patterson, "Optimizing coherence in 1-D noisy consensus networks with noise-free leaders," in *Proc. Amer. Control Conf.*, Seattle, WA, USA, May 2017, pp. 3011–3016.

[18] K. Fitch and N. E. Leonard, "Joint centrality distinguishes optimal leaders in noisy networks," *IEEE Trans. Control Netw. Syst.*, vol. 3, no. 4, pp. 366–378, Dec. 2016.

[19] M. Fardad, F. Lin, and M. R. Jovanović, "Algorithms for leader selection in large dynamical networks: Noise-free leaders," in *Proc. 50th IEEE Conf. Decis. Control Eur. Control Conf.*, Orlando, FL, USA, Dec. 2011, pp. 7188–7193.

[20] H. Kawashima and M. Egerstedt, "Leader selection via the manipulability of leader-follower networks," in *Proc. Amer. Control Conf.*, Montreal, QC, Canada, Jun. 2012, pp. 6053–6058.

[21] S. Patterson, "In-network leader selection for acyclic graphs," in *Proc. Amer. Control Conf.*, Chicago, IL, USA, Jan. 2015, pp. 329–334.

[22] F. Bullo, J. Cortés, and S. Martínez, *Distributed Control of Robotic Networks* (Applied Mathematics Series). Princeton, NJ, USA: Princeton Univ. Press, 2009.

[23] I. Shames, A. M. H. Teixeira, H. Sandberg, and K. H. Johansson, "Distributed leader selection without direct inter-agent communication," in *Proc. 2nd IFAC Work. Estimation Control Netw. Syst.*, Annecy, France, Sep. 2010, pp. 221–226.
[24] A. Franchi and P. Robuffo Giordano, "Online leader selection for improved collective tracking and formation maintenance," *IEEE Trans. Control Netw. Syst.*, vol. 5, no. 1, pp. 3–13, Mar. 2018.
[25] W. Ren, "Consensus seeking in multi-vehicle systems with a time-varying reference state," in *Proc. Amer. Control Conf.*, New York, NY, USA, Jul. 2007, pp. 717–722.
[26] P. Yang, R. A. Freeman, G. J. Gordon, K. M. Lynch, S. S. Srinivasa, and R. Sukthankar, "Decentralized estimation and control of graph connectivity for mobile sensor networks," *Automatica*, vol. 46, no. 2, pp. 390–396, 2010.
[27] R. A. Freeman, P. Yang, and K. M. Lynch, "Stability and convergence properties of dynamic average consensus estimators," in *Proc. 45th IEEE Conf. Decis. Control*, San Diego, CA, USA, Jan. 2006, pp. 338–343.
[28] B. Briegel, D. Zelazo, M. Burger, and F. Allgöwer, "On the zeros of consensus networks," in *Proc. 50th IEEE Conf. Decis. Control*, Orlando, FL, USA, Dec. 2011, pp. 1890–1895.

Antonio Franchi (S'07–M'11–SM'16) received the Ph.D. degree in system engineering from Sapienza University of Rome, Rome, Italy, in 2010.

In 2009, he was a Visiting Scholar with the University of California at Santa Barbara, Santa Barbara, CA, USA. From 2010 to 2014, he was a Research Scientist, a Senior Research Scientist, and the Project Leader of the Autonomous Robotics and Human Machine Systems Group, Max Planck Institute for Biological Cybernetics, Tübingen, Germany. Since 2014, he has been a CNRS Researcher with the RIS team, LAAS-CNRS, Toulouse, France.

Dr. Franchi is a founding Co-Chair of the IEEE RAS Technical Committee on Multiple Robot Systems.

Paolo Robuffo Giordano (M'08–SM'16) received the M.Sc. degree in computer science engineering and the Ph.D. degree in systems engineering from the University of Rome "La Sapienza," Rome, Italy, in 2001 and 2008, respectively.

In 2007 and 2008, he spent one year as a Postdoctoral Researcher with the Institute of Robotics and Mechatronics of the German Aerospace Center (DLR), and from 2008 to 2012, he was Senior Research Scientist with the Max Planck Institute for Biological Cybernetics, Tübingen, Germany. He is currently a Senior CNRS Researcher Head of the Rainbow group, Irisa and Inria, Rennes, France.

Giulia Michieletto (M'18) received the Master's degree in automation engineering and the Ph.D. degree in information engineering from the University of Padova, Padua, Italy, in 2014 and 2017, respectively.

From 2016 to 2017, she was a Visiting Researcher with LAAS-CNRS, Toulouse, France, working on the RIS team under the supervision of Antonio Franchi. Since 2018, she has been a Postdoctoral Fellow with the SPARCS Group, University of Padova. Her main research interests include multiagent systems modeling and control with a special regard to networked formations of aerial vehicles and nano satellites.